This full text paper was peer reviewed at the direction of IEEE Communications Society subject matter experts for publication in the WCNC 2010 proceedings.

Training Sequence-aided Single-carrier Block Signal Detection Using QRM-MLD

Tetsuya YAMAMOTO† Kazuki TAKEDA† and Fumiyuki ADACHI‡
Dept. of Electrical and Communication Engineering, Graduate School of Engineering, Tohoku University
6-6-05 Aza-Aoba, Aramaki, Aoba-ku, Sendai, 980-8579 Japan
†{yamamoto, kazuki}@mobile.ecei.tohoku.ac.jp, ‡adachi@ecei.tohoku.ac.jp

Abstract—**Recently, we proposed a frequency-domain block signal detection using maximum likelihood detection (MLD) employing QR decomposition and M-algorithm (QRM-MLD) for the cyclic prefix inserted single-carrier (CP-SC) block transmissions. However, if the number of surviving-symbol candidates is small, the achievable bit error rate (BER) performance degrades, because the probability of removing the correct symbol-candidates at early stages increases. In this paper, to solve this problem, we insert the known training sequence into each data block instead of CP. This SC transmission is called the training sequence-aided SC (TA-SC) block transmissions. We show by computer simulation that the TA-SC can achieve much better BER performance than the CP-SC if the number of surviving symbol-candidates is limited.**

Keywords-component; Single-carrier, QRM-MLD, training sequence

I. INTRODUCTION

In next generation mobile communication systems, broadband data services are demanded. Since the mobile wireless channel is composed of many propagation paths with different time delays, the channel becomes severely frequency-selective as the transmission data rate increases. When single-carrier (SC) transmission without equalization technique is used, the bit error rate (BER) performance significantly degrades due to inter-symbol interference (ISI) [1]. A cyclic prefix inserted SC (CP-SC) block transmission with simple one-tap frequency-domain equalization (FDE) based on the minimum mean square error criterion (MMSE) can significantly improve the BER performance in a frequency-selective fading channel [2, 3]. However, due to the presence of residual ISI after FDE, a big performance gap exists from the matched filter bound (MF bound) [4]. To narrow the performance gap, a frequency-domain iterative ISI cancellation technique combined with MMSE-FDE was proposed in [4, 5]. However, the achievable BER performance is still a few dB away from the MF bound.

Recently, we proposed a frequency-domain block signal detection using maximum likelihood detection (MLD) employing QR decomposition and M-algorithm (called QRM-MLD) [6] for the CP-SC block transmissions. We showed that the QRM-MLD frequency-domain block signal detection significantly improves the BER performance compared to the MMSE-FDE and achieves BER performance close to the MF bound by increasing the number of surviving symbol-candidates. However, if the number of surviving-symbol candidates is small, the achievable BER performance degrades because the probability of removing the correct symbol-candidates at early stages increases. This probability of removing the correct symbol-candidates at early stages affects greatly the achievable BER of QRM-MLD.

If the symbols to be detected at early stages are known, the achievable BER performance of QRM-MLD can be improved. The training sequence-aided SC (TA-SC) block transmission [7, 8] was proposed to achieve simple synchronization and fast tracking against channel variations. In TA-SC, the training sequence in the previous block acts as the CP in the present block. This can be exploited for the QRM-MLD frequency-domain block signal detection to reduce the probability of removing the correct symbol-candidates at early stages. In this paper, we show by computer simulation that the TA-SC system using QRM-MLD frequency-domain block signal detection can achieve close to the MF bound while reducing the number of surviving symbol-candidates.

The remainder of this paper is organized as follows. In Sect. II, the TA-SC system using QRM-MLD frequency-domain block signal detection is presented. Sect. III discusses the computer simulation results. Sect. IV offers the conclusion.

II. TA-SC USING QRM-MLD FREQUENCY-DOMAIN BLOCK SIGNAL DETECTION

A. *TA-SC vs CP-SC*

The block structure of the TA-SC transmissions is illustrated and compared to CP-SC in Fig. 1. The basic idea of the TA-SC is to replace the CP in a training sequence. For the CP-SC block transmissions, the number of useful data symbols and the length of the CP are respectively denoted by N_c and N_g. For the TA-SC transmissions, to achieve the same data rate as the CP-SC, the useful data symbol sequence of length N_c and the training sequence of length N_g are used. The difference between TA-SC and CP-SC is the size of discrete Fourier transform (DFT) to be used at the receiver; the DFT size is N_c symbols for the CP-SC and is N_c+N_g symbols for TA-SC.

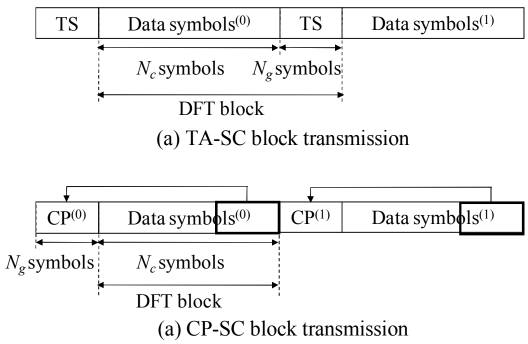

Figure 1. Block structure.

B. Trasnmited Signal

Throughout the paper, the symbol-spaced discrete time representation is used. At the transmitter, a binary information sequence is data-modulated and then is divided in to a sequence of block of N_c data symbols each. Before the transmission, the training sequence of length N_g symbols is appended at the end of each block. The transmitted block $\mathbf{x}$ is expressed using the vector form as

$$\begin{aligned}\mathbf{x} &= [x(0),...,x(N_c+N_g-1)]^T \\ &= [d(0),...,d(N_c-1),u(0),...,u(N_g-1)]^T , \\ &= [\mathbf{d}^T \quad \mathbf{u}^T]^T\end{aligned} \tag{1}$$

where $\mathbf{d}=[d(0),\ldots,d(N_c-1)]^T$ and $\mathbf{u}=[u(0),\ldots,u(N_g-1)]^T$ denote respectively the data symbol vector and the training sequence vector which is the same for all blocks.

C. Received Signal

We assume a symbol-spaced frequency-selective fading channel composed of L distinct propagation paths. The channel impulse response $h(\tau)$ is given by

$$h(\tau)=\sum_{l=0}^{L-1} h_l \delta(\tau-\tau_l) , \tag{2}$$

where h_l and τ_l are respectively the complex-valued path gain with $E[\sum_{l=0}^{L-1}|h_l|^2]=1$ and the time delay of the lth path. We assume the lth path time delay is l symbols, i.e. ($\tau_l=l$). The received signal block $\mathbf{y}=[y(0),...,y(N_c+N_g-1)]^T$ can be expressed using the vector form as

$$\mathbf{y}=\sqrt{\frac{2E_s}{T_s}}\mathbf{hx}+\mathbf{n} . \tag{3}$$

where E_s and T_s are respectively the symbol energy and the symbol duration, $\mathbf{h}$ is the $(N_c+N_g)\times(N_c+N_g)$ channel impulse response matrix given as

$$\mathbf{h}=\begin{bmatrix} h_0 & & & & & h_{L-1} & & \\ \vdots & h_0 & & & & & \ddots & \\ & \vdots & h_0 & \mathbf{0} & & & & h_{L-1} \\ h_{L-1} & & \vdots & \ddots & & & & \\ & h_{L-1} & & & h_0 & & & \\ & & h_{L-1} & & \vdots & \ddots & & \\ \mathbf{0} & & & \ddots & & & & h_0 \end{bmatrix}, \tag{4}$$

and $\mathbf{n}=[n(0),...,n(N_c+N_g-1)]^T$ is the noise vector. The tth element, $n(t)$, of $\mathbf{n}$ is the zero-mean additive white Gaussian noise (AWGN) having the variance $2N_0/T_s$ with N_0 being the one-sided noise power spectrum density.

D. Frequency-domain Received Signal

(N_c+N_g)-point DFT is applied to transform the received signal block into the frequency-domain signal vector $\mathbf{Y}=[Y(0),\ldots,Y(N_c+N_g-1)]^T$. $\mathbf{Y}$ is expressed as

$$\mathbf{Y}=\mathbf{Fy}=\sqrt{\frac{2E_s}{T_s}}\mathbf{Fhx}+\mathbf{Fn} , \tag{5}$$

where $\mathbf{F}$ is the DFT matrix of size $(N_c+N_g)\times(N_c+N_g)$ given by

$$\mathbf{F}=\frac{1}{\sqrt{N_c+N_g}}\begin{bmatrix} 1 & 1 & \cdots & 1 \\ 1 & e^{-j2\pi\frac{1\times1}{N_c+N_g}} & \cdots & e^{-j2\pi\frac{1\times(N_c+N_g-1)}{N_c+N_g}} \\ \vdots & \vdots & \ddots & \vdots \\ 1 & e^{-j2\pi\frac{(N_c+N_g-1)\times1}{N_c+N_g}} & \cdots & e^{-j2\pi\frac{(N_c+N_g-1)\times(N_c+N_g-1)}{N_c+N_g}} \end{bmatrix}. \tag{6}$$

Due to the circulant property of $\mathbf{h}$ [9], we have

$$\mathbf{FhF}^H = diag[H(0),\ldots,H(N_c+N_g-1)] \equiv \mathbf{H} , \tag{7}$$

where $H(k)=\sum_{l=0}^{L-1} h_l \exp(-j2\pi k\tau_l/(N_c+N_g))$, $k=0\sim N_c+N_g-1$, and $(.)^H$ is the Hermitian transpose operation. Using Eq. (7), Eq. (5) can be rewritten as

$$\mathbf{Y}=\sqrt{\frac{2E_s}{T_s}}\mathbf{HFx}+\mathbf{N}=\sqrt{\frac{2E_s}{T_s}}\overline{\mathbf{H}}\mathbf{x}+\mathbf{N} , \tag{8}$$

where $\overline{\mathbf{H}}=\mathbf{HF}$ and $\mathbf{N}=[N(0),...,N(N_c+N_g-1)]^T$ are respectively the equivalent channel matrix and the frequency-domain noise vector.

E. QRM-MLD

In the case of SC transmissions, all symbols have the same signal-to-interference plus noise power ratio (SINR) and hence, no ordering is necessary. First, applying the QR decomposition to the equivalent channel matrix $\overline{\mathbf{H}}$, we have $\overline{\mathbf{H}}=\mathbf{QR}$, where $\mathbf{Q}$ is an $(N_c+N_g)\times(N_c+N_g)$ matrix satisfying $\mathbf{Q}^H\mathbf{Q}=\mathbf{I}$ and $\mathbf{R}$ is an $(N_c+N_g)\times(N_c+N_g)$ upper triangular matrix. The transformed frequency-domain received signal $\hat{\mathbf{Y}}=[\hat{Y}(0),...,\hat{Y}(N_c-1),\hat{Y}(N_c),...,\hat{Y}(N_c+N_g-1)]^T$ is obtained as

$$\hat{\mathbf{Y}} = \mathbf{Q}^H\mathbf{Y} = \sqrt{\frac{2E_s}{T_s}}\mathbf{R}\mathbf{x} + \mathbf{Q}^H\mathbf{N}$$
$$= \sqrt{\frac{2E_s}{T_s}}\begin{bmatrix} R_{0,0} & \cdots & R_{0,N_c-1} & R_{0,N_c} & \cdots & R_{0,N_c+N_g-1} \\ & \ddots & \vdots & \vdots & \ddots & \vdots \\ & & R_{N_c-1,N_c-1} & R_{N_c-1,N_c} & \cdots & R_{N_c-1,N_c+N_g-1} \\ & & & R_{N_c,N_c} & \cdots & R_{N_c,N_c+N_g-1} \\ & \mathbf{0} & & & \ddots & \vdots \\ & & & & & R_{N_c+N_g-1,N_c+N_g-1} \end{bmatrix}\begin{bmatrix} d(0) \\ \vdots \\ d(N_c-1) \\ u(0) \\ \vdots \\ u(N_g-1) \end{bmatrix} + \mathbf{Q}^H\mathbf{N} \quad (9)$$

The M-algorithm [10] is composed of N_c+N_g stages with each stage detecting one of N_c+N_g symbols in a block. In the nth stage, the metric based on the squared Euclidian distance associated with each of symbol-candidates for symbol $d(N_c-1-n)$ is calculated using the nth element of $\hat{\mathbf{Y}}$ and the element of the nth row of $\mathbf{R}$. The best M symbol-candidates are selected by comparing the metrics of all candidates as surviving symbol-candidates and are passed to the next stage. However, since the N_c~(N_c+N_g-1)th elements in $\hat{\mathbf{Y}}$ contain the training symbols only, the 0~(N_g-1)th stages can be skipped. The M-algorithm can be started from N_g stage.

In the N_gth stage, all possible symbol candidates for the last symbol $d(N_c-1)$ are generated (for example, the number of all possible symbol-candidates are 4 and 16 for QPSK and 16QAM, respectively). The metric based on the squared Euclidian distance between $\hat{Y}(N_c-1)$ and each symbol candidate is calculated as

$$e_{N_g} = \left|\hat{Y}(N_c-1) - \sqrt{\frac{2E_s}{T_s}}R_{N_c-1,N_c-1}\bar{d}(N_c-1)\right|^2, \quad (10)$$

where $\bar{d}(n)$ is the symbol candidates for $d(n)$. Then, M ($M \le X$) symbol-candidates having the smallest metrics are selected as surviving symbol candidates, where X is the modulation level (e.g. X=4 and 16 for QRSK and 16QAM, respectively). These surviving symbol-candidates are transferred to the next stage. In the N_g+1 stage, there are a total of X symbol-candidates of $d(N_c-2)$ leaving from each of surviving symbol-candidate of $d(N_c-1)$. Therefore, there are a total of $M \cdot X$ combinations of $d(N_c-1)$ and $d(N_c-2)$. The metrics are calculated for all possible $M \cdot X$ combinations using

$$e_{N_g+1} = \sum_{n=0}^{1}\left|\hat{Y}(N_c-1-n) - \sqrt{\frac{2E_s}{T_s}}\sum_{i=0}^{n}R_{N_c-1-n,N_c-1-i}\bar{d}(N_c-1-i)\right|^2 . \quad (11)$$

Similar to the N_g stage, M surviving symbol-candidates are selected from $M \cdot X$ combinations of $d(N_c-1)$ and $d(N_c-2)$. This process is repeated until the last stage. Signal detection is carried out using the symbol-candidate with the smallest metric at the last stage.

F. *Advantage of TA-SC*

The received signal power associated with the symbol $d(N_c-1-n)$ to be detected at the n'th stage ($n' \ge n+N_g$, n=0~N_c −1) is the sum of the squared values of the (N_c-1-n')~(N_c-1)th elements in the (N_c-1-n)th column of $\mathbf{R}$. Since the channel impulse response matrix is a circulant matrix, the squared values of the diagonal element of $\mathbf{R}$ closer to the lower right positions likely drop [11]. In the case of the TA-SC transmissions, the elements of $\mathbf{R}$ closer to lower right positions are associated with the training sequence and therefore these elements are not relevant to the detection of the useful data symbols. On the other hand, in the case of the CP-SC transmissions, the elements of $\mathbf{R}$ closer to lower right positions have an effect on the detection of the useful data symbols since the transformed frequency-domain received signal $\hat{\mathbf{Y}}^{(CP)} = [\hat{Y}(0),...,\hat{Y}(N_c-1)]^T$ is obtained as

$$\hat{\mathbf{Y}}^{(CP)} = \sqrt{\frac{2E_s}{T_s}}\mathbf{R}^{(CP)}\mathbf{d} + \mathbf{Q}^H\mathbf{N}^{(CP)}$$
$$= \sqrt{\frac{2E_s}{T_s}}\begin{bmatrix} R_{0,0}^{(CP)} & R_{0,1}^{(CP)} & \cdots & R_{0,N_c-1}^{(CP)} \\ & R_{1,1}^{(CP)} & \cdots & R_{1,N_c-1}^{(CP)} \\ & & \ddots & \vdots \\ & & & R_{N_c-1,N_c-1}^{(CP)} \end{bmatrix}\begin{bmatrix} d(0) \\ d(1) \\ \vdots \\ d(N_c-1) \end{bmatrix} + \mathbf{Q}^H\mathbf{N}^{(CP)} \quad (12)$$

When small M is used, the probability of removing the correct symbol-candidates at an earlier stage may increase because the elements of $\mathbf{R}$ closer to lower right positions are relevant to the detection of the useful data symbols. The selection error at an earlier stage affects the achievable BER performance of QRM-MLD greatly since the MLD based on the M-algorithm successively reduces the symbol-candidate stage-by-stage. Therefore, to improve the BER performance, the probability of removing the correct symbol-candidates at an earlier stage must be reduced.

The use of a large M is necessary in order to achieve the performance close to the MF bound. For example, M=256 is necessary for 16QAM modulation when N_c=64 [6]. The use of larger M increases the computational complexity. However, in the case of the TA-SC transmissions, the M-algorithm can start from the n=N_gth stage and therefore, the probability of removing the correct symbol-candidates at an earlier stage can be reduced even if small M is used. This suggests that the value of M can be reduced in the TA-SC transmissions.

III. Computer Simulation

The simulation condition is shown in Table I. The number of useful data symbols is N_c=64 symbols for both TA- and CP-SC and the training sequence for the TA-SC is N_g=16 symbols which is equal to the CP length of the CP-SC. A partial sequence taken from a PN sequence with a repetition period of 4095 bits is used as the training sequence $\mathbf{u}$. The modulation of

This full text paper was peer reviewed at the direction of IEEE Communications Society subject matter experts for publication in the WCNC 2010 proceedings.

training sequence is the same as data sequence. The channel is assumed to be a frequency-selective block Rayleigh fading channel having symbol-spaced L=16-path uniform power delay profile. Ideal channel estimation is assumed.

TABLE I. COMPUTER SIMULATION CONDITION

Transmitter	Modulation	QPSK, 16QAM
	The number of useful data symbols	N_c=64
	Length of TS or CP	N_g=16
Channel	Fading type	Frequency-selective block Rayleigh
	Power delay profile	L=16-path uniform power delay profile
	Time delay	$\tau_l=l$ (l=0~L−1)
Receiver	Channel estimation	Ideal

The average BER performance of the TA-SC using QRM-MLD frequency-domain block signal detection is plotted in Fig. 2 as a function of average received bit energy-to-noise power spectrum density ratio $E_b/N_0(=(E_s/N_0)(1+N_g/N_c)/\log_2 X)$, where X denotes the modulation level. Three cases are plotted, i.e., M=1, 4, and 8 for QPSK and M=1, 4, and 16 for 16QAM. For comparison, the CP-SC performance and the MF bound [12] are plotted. When small M is used, the achievable BER performance of the CP-SC degrades because the probability of removing the correct symbol-candidates at an early stage increases. On the other hand, the TA-SC can achieve better BER even if small M is used. The reason for this is discussed below.

Figure 3 shows the probability density function (pdf) of the squared value of R_{N_c-1,N_c-1} and $R^{(CP)}_{N_c-1,N_c-1}$ (the received signal power associated with the symbol to be detected at the N_g stage for TA-SC and first stage for CP-SC). It is seen that when the CP-SC is used, the probability that the received signal power drops is high and therefore, the probability of removing the correct symbol-candidates at first stages increases when small M is used. On the other hand, the TA-SC does not use the rows near bottom of $\mathbf{R}$ and therefore, the probability of removing the correct symbol-candidates at the earlier stages can be reduced.

Figure 4 plots the required E_b/N_0 for achieving BER=10^{-3} as a function of M. For comparison, the required E_b/N_0 obtained from the MF bound is also plotted. The CP-SC requires M larger than 64(256) for QPSK(16QAM) to achieve the BER performance close to the MF bound. However, the TA-SC requires much smaller M (i.e., M=8(16) for QPSK(16QAM)). The performance gap of 0.97dB from the MF bound is owing to the loss due to the insertion of CP and training sequence.

The computational complexities of the QRM-MLD frequency-domain block signal detection for the TA-SC and the CP-SC is compared in terms of the number of complex multiplications. First, we discuss the number of matrix multiplications required for the squared Euclidian distance calculations. The number of multiplications required for the squared Euclidian distance calculations is $X\{2+(M/2)(N_c+4)(N_c-1)\}$. For QPSK(16QAM), the TA-SC can reduce the value of M by 1/8(1/16) compared to the CP-SC, and hence the computational complexity of the TA-SC is about 13(8)% of the CP-SC.

Next, we discuss the overall computational complexity. The number of multiplications is given in Table II. The TA-SC requires higher complexity to get the frequency-domain signal since DFT is required instead of FFT and also requires higher complexity for QR decomposition and multiplication of $\mathbf{Q}^H$ (this is because the size of equivalent channel matrix is larger than that of the CP-SC). However, the TA-SC can reduce the complexity significantly required for the squared Euclidian distance calculations. As a result, the overall complexity of the TA-SC is smaller than the CP-SC and is about 73(12)% when QPSK(16QAM) is used. The computational complexity relative to the CP-SC reduces for higher modulation level X.

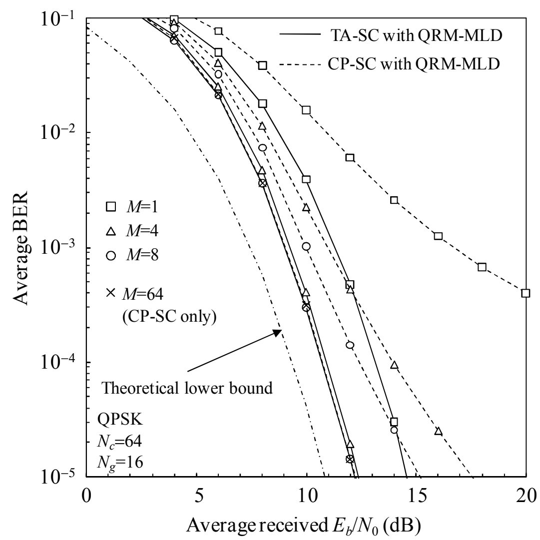

(a) QPSK

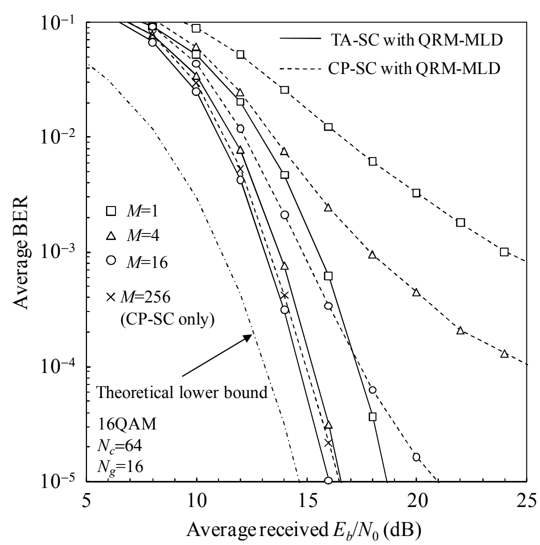

(b) 16QAM

Figure 2. Average BER performance.

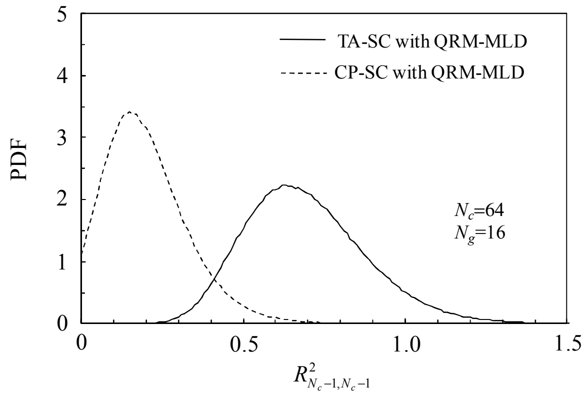

Figure 3. PDF of $R^2_{N_c-1,N_c-1}$.

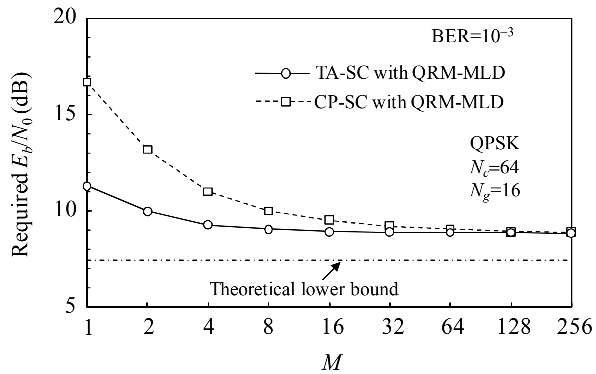

(a) QPSK

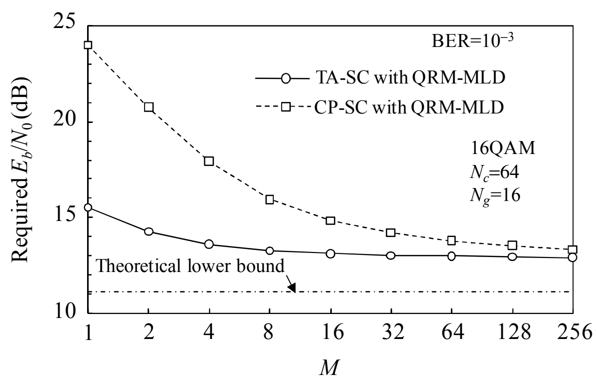

(b) 16QAM

Figure 4. Required average received E_b/N_0 as a function of the number M of surviving symbol-candidates.

TABLE II. NUMBER OF MULTIPLICATIONS

	TA-SC with QRM-MLD	CP-SC with QRM-MLD
FFT or DFT	$(N_c+N_g)^2$	$N_c \times \log_2 N_c$
QR decomposition	$(N_c+N_g)^3$	N_c^3
Multiplication of $\mathbf{Q}^H$	$(N_c+N_g)^2$	N_c^2
Squared Euclidian distance calculations	$X\{2+(M/2)(N_c+4)(N_c-1)\}$	$X\{2+(M/2)(N_c+4)(N_c-1)\}$

IV. CONCLUSIONS

In this paper, we presented the QRM-MLD frequency-domain block signal detection for the TA-SC signal transmissions, in which the training sequence in the previous block acts as the CP in the present block. We incorporated the known training sequence into the M-algorithm to reduce the probability of removing the correct symbol-candidates at early stages. We showed by computer simulation that the TA-SC system can achieve the BER performance close to the MF bound while reducing the computational complexity. When 16QAM is used, the TA-SC reduces the overall complexity by about 12%.

In this paper, ideal channel estimation was assumed. The performance comparison between TA-SC and CP-SC in the presence of channel estimation errors is left for future study.

REFERENCES

[1] J. G. Proakis and M. Salehi, *Digital communications*, 5th ed., McGraw-Hill, 2008.

[2] D. Falconer, S. L. Ariyavisitakul, A. Benyamin-Seeyar B. Edison, "Frequency domain equalization for single-carrier broadband wireless systems," IEEE Commun. Mag., Vol. 40, No. 4, pp. 58-66. Apr. 2002.

[3] K. Takeda, T. Itagaki, and F. Adachi, "Joint use of frequency-domain equalization and transmit/receive antenna diversity for single-carrier transmissions," IEICE Trans. Commun., vol. E87-B, No. 7, pp.1946-1953, Jul. 2004.

[4] N. Benvenuto and S. Tomasin, "Block iterative DFE for single carrier modulation," Electron. Lett., Vol. 38, No. 19, pp. 1144-1145, Sep. 2002.

[5] K. Takeda, K. Ishihara and F. Adachi, "Frequency-domain ICI cancellation with MMSE equalization for DS-CDMA downlink," IEICE Trans. Commun., Vol. E89-B, No. 12, pp. 3335-3343, Dec. 2006.

[6] T. Yamamoto, K. Takeda, and F. Adachi, "Single-carrier transmission using QRM-MLD with antenna diversity," The 12th International Symposium on Wireless Personal Multimedia Communications (WPMC 2009), Sendai, Japan, Sept. 2009.

[7] L. Deneire, B. Gyselinckx, and M. Engels, "Training sequence versus cyclic prefix - a new look on single carrier communication," IEEE Commun. Lett., Vol. 5, No. 7, pp. 292-294, July, 2001.

[8] J. Coon, M. Sandell, M. Beach and J. McGeehan, "Channel and noise variance estimation and tracking algorithms for unique-word based single-carrier systems," IEEE Trans. on Wireless Commun., Vol. 5, No. 6, pp. 1488-1496, June 2006.

[9] G. H. Golub and C. F. van Loan, *Matrix Computations*, 3rd ed. Baltimore, MD, Johns Hopkins Univ. Press, 1996.

[10] J. B. Anderson and S. Mohan, "Sequential coding algorithms: A survey and cost analysis," IEEE Trans. on Commun., Vol. 32, pp. 169-176, Feb. 1984.

[11] K. Takeda, H. Tomeba, and F. Adachi, "Joint Tomlinson-Harashima precoding and frequency-domain equalization for broadband single-carrier transmission," IEICE Trans. Commun., V0l. 91-B, No. 1, pp. 258-266, Jan. 2008.

[12] F. Adachi and K. Takeda, "Bit error rate analysis of DS-CDMA with joint frequency-domain equalization and antenna diversity combining," IEICE Trans. Commun., vol. E87-B, No. 10, pp.2991-3002, Oct. 2004.